A CASPT2//CASSCF Study of Vertical and Adiabatic Electron Transitions of Acrolein in Water Solution

Aurora Muñoz Losa, Ignacio Fdez. Galván, Manuel A. Aguilar, and M. Elena Martín*

Dpto. Química Física. Universidad de Extremadura, Avda. de Elvas s/n, 06071 Badajoz, Spain

Received: March 12, 2007; In Final Form: May 23, 2007

The $^1(n \rightarrow \pi^*)$ excited-state of acrolein in liquid water was studied theoretically by using the averaged solvent electrostatic potential from molecular dynamics method (ASEP/MD). The model combines a multireference perturbational CASPT2//CASSCF treatment in the description of the solute molecule with NVT molecular dynamics simulations in the description of the solvent. In this paper, we present two alternative methods for calculating solvent shift on adiabatic transitions and their performance is analyzed. In the first method, the free energy change during an adiabatic transition is calculated classically by using the free energy perturbation method. In the second method, it is calculated from the quantum values of the vertical absorption and emission electron transition energies. The $^1(n \rightarrow \pi^*)$ excitation is accompanied by a charge flux from the oxygen to the carbon skeleton, this charge flux decreases the dipole moment of the excited-state with respect to the ground state value and, consequently, the solute−solvent interaction energy. This effect destabilizes the excited-state with respect to the ground state and produces a blue shift in the absorption and emission bands. For the emission process, there also exists an additional destabilization due to a partial desolvation of the excited state. The effect of the solvent electron polarization, the inclusion of the solute electron correlation, and the use of relaxed geometries in solution on the calculated solvent shift of the absorption and emission spectra are also analyzed.

Introduction

Although the theoretical study of solvent effects on UV/vis spectra has a long history and has been profusely treated in the literature,[1] most papers published to date have been dedicated to the study of vertical absorption spectra; comparatively less attention has been paid to the study of solvent effects on emission spectra and adiabatic transitions (transitions between states at distinct regions of the free energy surface). Probably, one of the causes of this scarcity is the difficulty for obtaining excited-state geometries in solution with the adequate precision. Diverse studies[2] have shown that highly accurate quantum methods, such as CASPT2 (complete active space with second-order perturbation theory) or MRPT2 (second-order multireference perturbation theory), and very precise geometrical parameters must be used to obtain an appropriate description of the electron spectra of molecules in gas phase. Furthermore, in solution, we must have a precise description of the solvent effects available. Traditionally, most studies have used some version of the dielectric continuum method.[3] Although these methods can provide, in a wide variety of cases, an adequate description of the solvent, they can fail when specific solute−solvent interactions are involved, as it is the case, for instance, with hydrogen-bonded systems.

In the present paper, we extend a method, previously employed in the study of electron absorption spectra,[4] to the case of emission and adiabatic transitions. The method, known as ASEP/MD,[5] introduces the averaged solvent electrostatic potential (ASEP) obtained through molecular dynamics (MD) into the molecular Hamiltonian of the chromophore and combines the high level quantum calculations needed in the description of the chromophore with a detailed description of the solvent obtained from simulations. As a test case, we have chosen acrolein in water solution. Acrolein or propenal is the smallest α,β-unsaturated carbonyl compound. The interaction between the carbonyl group and the C=C double bond makes it a compound of marked interest from a spectroscopic and theoretical point of view. Furthermore it has been shown that it can form several hydrogen bonds with the water molecules. Its electronic spectrum has been extensively studied[6] by different spectroscopic techniques. The UV-spectrum of this compound has also been studied theoretically with ab initio[7] and semiempirical methods,[8,9] and both the lowest excited states and the high-energy part of the electronic spectrum have been characterized. The effect of solvation on the absorption spectrum has also been theoretically studied by using a supermolecule approach[8] and with the RISM-SCF method[9] and, more recently, with continuum models,[10] with quantum mechanics/molecular mechanics (QM/MM) models,[11] and with ASEP/MD.[12] Concerning the evolution of the excited state, the time dependent Stokes shift has recently been determined using a extended version of the PCM method.[13] However, to our knowledge, no intent has been done for the theoretical characterization of the in solution emission spectrum.

Method

ASEP/MD is a QM/MM effective Hamiltonian method that makes use of the mean field approximation,[5] that is, it introduces, into the solute molecular Hamiltonian, the averaged perturbation generated by the solvent. The method combines quantum mechanics (QM) and molecular mechanics (MM) techniques, with the particularity that full QM and MM calculations are alternated and not simultaneous. During the MD

* Corresponding author e-mail: memartin@unex.es.

10.1021/jp071993r CCC: $37.00
Published on Web 08/01/2007

simulations, the intramolecular geometry and charge distribution of all the molecules are considered as fixed. From the resulting data, the average electrostatic potential generated by the solvent on the solute is obtained. This potential is introduced as a perturbation into the solute's quantum mechanical Hamiltonian, and by solving the associated Schrödinger equation, one gets a new charge distribution for the solute, which is used in the next MD simulation. The iterative process is repeated until the electron charge distribution of the solute and the solvent structure around it are mutually equilibrated. The main characteristics of the method have been described elsewhere.[5] Here, we shall detail only some points pertinent to the current study.

Geometry Optimization of Excited States. The solute excited-state geometry in presence of the solvent was optimized using a technique described in a previous paper[13] and based on the use of the free-energy gradient method.[14] The technique has been successfully applied to geometry optimization of molecular ground states in solution. At each step of the optimization procedure the mean value of the total force, F, and the Hessian, H, of the excited-state averaged over a representative set of solvent configurations were calculated as the sum of the solute and solvent contributions and were used to obtain a new geometry by using the rational function optimization method. The force and Hessian read[13]

$$F(r) = -\frac{\partial G(r)}{\partial r} = -\left\langle \frac{\partial V(r,X)}{\partial r} \right\rangle \approx -\frac{\partial \langle V(r,X)\rangle}{\partial r} \quad (1)$$

$$H(r,r') \approx \frac{\partial^2 \langle V(r,X)\rangle}{\partial r \partial r'} \quad (2)$$

where $G(r)$ is the free energy, $V(r,X)$ is a potential energy, sum of intra- and intermolecular (solute−solvent) contributions, and the brackets denote a statistical average over the solvent configurations, X.

Transition Energies. Once we determined the geometries and wave function of the initial, (*i*), and final, (*f*), solute states in solution, we proceeded to the determination of the free energy difference between the two states considered. The standard free-energy difference between "*i*" and "*f*" states in solution, the transition energy, can be written as sum of two terms:[15]

$$\Delta G_{\text{diff}} = \Delta E_{\text{solute}} + \Delta G_{\text{int}} \quad (3)$$

where

$$\Delta E_{\text{solute}} = E^f - E^i = \langle \psi^f \mid \hat{H}_{\text{QM}} \mid \psi^f \rangle - \langle \psi^i \mid \hat{H}_{\text{QM}} \mid \psi^i \rangle \quad (4)$$

is the ab initio difference between the two quantum mechanics, QM, states (excited and ground state in this case) calculated using the in vacuo solute molecular Hamiltonian, $\hat{H}_{\text{QM}}$, and the electronic wave functions obtained in solution by solving the following Schrödinger equation:

$$(\hat{H}_{\text{QM}} + \hat{H}^{\text{elect}}_{\text{QM/MM}}) \mid \psi\rangle = E \mid \psi\rangle \quad (5)$$

$$\hat{H}^{\text{elect}}_{\text{QM/MM}} = \int dr \cdot \hat{\rho} \cdot V_{\text{ASEP}}(r) \quad (6)$$

where $V_{\text{ASEP}}(r)$ is the averaged electrostatic potential generated by the solvent, that in general depends on the solute state. Details about the calculation of $V_{\text{ASEP}}(r)$ can be found elsewhere.[5] $\hat{\rho}$ is the charge density operator of the solute. The solute−solvent Lennard-Jones contribution is added to the energy a posteriori and hence has no effect on the solute wave function; obviously, it contributes to the final value of the gradient and Hessian.

In eq 3, ΔG_{int} is the difference in the solute−solvent interaction free energy between the two QM states. This term can be calculated by using the free-energy perturbation (FEP) method.[16] An example of application of these techniques to electron transitions can be found in Debolt and Kollman.[16a]

The ΔG_{int} term can be split into two terms, $\Delta G_{\text{int}} = \Delta E_{\text{int}} + \Delta G_{\text{sol}}$ and hence the transition energy reads as follows:

$$\Delta G_{\text{diff}} = \Delta E_{\text{solute}} + \Delta E_{\text{int}} + \Delta G_{\text{sol}} \quad (7)$$

The last term, ΔG_{sol}, provides the solvent distortion energy, i.e., the energy spent in changing the solvent structure from the initial to the final state. The term ΔE_{int}, accounts for the difference in the solute−solvent interaction energy between the final and initial state. When the solvent is nonpolarizable the solute−solvent interaction energy difference is simply $\Delta E_{\text{int}} = \langle \psi^f | V^f_{\text{ASEP}} | \psi^f \rangle - \langle \psi^i \mid V^i_{\text{ASEP}} | \psi^i \rangle$. Furthermore, for vertical transitions, $V^f_{\text{ASEP}} = V^i_{\text{ASEP}}$. When the solvent is polarizable, the energy spent in polarizing the electron degrees of freedom of the solvent must also be included, see below. Strictly, part of this electron distortion energy of the solvent should be included into the ΔG_{sol} term, however, due to computational considerations, we prefer to include the contribution associated to the solvent electron displacement into the ΔE_{int} term, and we reserve ΔG_{sol} for the energy spent in the modification of the solvent structure that implies molecular rotation or translation. In this way ΔG_{sol} depends only on nuclear solvent coordinates.

When the solvent is polarizable, the determination of solvent shifts with the ASEP/MD method involves two steps. In the first one, the wave function and geometry of the solute are obtained for each state involved in the transition. During this first step the solvent structure around the solute is equilibrated, but it is supposed that the charge distribution of every solvent molecule remains fixed, that is, during the simulations one considers a nonpolarizable solvent. In the second step, the solvent structure is kept fixed but now the electron degrees of freedom of the solvent polarize in response to the changes in the solute charge distribution originated by the electron transition of the solute. That is, using the solvent structure and solute geometry obtained in the first step, we couple the quantum mechanical solute and the electron polarization of the solvent. To this end, we assign a molecular polarizability to every solvent molecule, and simultaneously, replace the effective solvent charge distribution used in the MD calculation (TIP3P for instance, if the solvent is water) with the gas-phase values of the solvent molecule. This is necessary because effective charges include a certain degree of implicit solvent polarization; when one considers a polarizable model, it is necessary to use the in vacuo charges of the solvent molecules to avoid accounting twice for this effect. This separation of the solvent effect in permanent and polarizable components is completely equivalent to that used in dielectric models where the solvent reaction field is sum of an orientational (or inertial) and an electronic (or dynamical) part.[16]

In previous papers,[4] we have shown that for a polarizable solvent, the solute−solvent interaction energy reads as follows:

$$E^{\text{pol}}_{\text{int}} = \frac{1}{2} U_{\mu q} + U_{\rho q} + \frac{1}{2} U_{\rho \mu} \quad (8)$$

Here, q refers to the permanent charges of solvent molecules, μ to the solvent induced dipoles, and ρ is the solute charge

density. As we indicate above E_{int} includes also the polarization energy of the solvent dipoles.

The transition energy is calculated applying eq 8 to the final and initial states, computing the difference and adding the rest of the terms of eq 7.

$$\Delta G_{diff}^{pol} = \Delta E_{solute} + \frac{1}{2}\Delta U_{\mu q} + \Delta U_{\rho q} + \frac{1}{2}\Delta U_{\rho\mu} + \Delta G_{sol} \quad (9)$$

Finally, the solvent shift, δ, can be calculated as the difference between the in solution and the in vacuo transition, ΔE_{solute}^{0},

$$\delta = \Delta G_{diff}^{pol} - \Delta E_{solute}^{0} = \Delta E_{solute}^{distortion} + \frac{1}{2}\Delta U_{\mu q} + \Delta U_{\rho q} + \frac{1}{2}\Delta U_{\rho\mu} + \Delta G_{sol} \quad (10)$$

In the case of vertical transitions the term ΔG_{sol} cancels out because the Franck−Condon approximation is applicable and the solvent structure is the same in both the ground and the excited state. Furthermore, the interaction energies, E_{int}^{pol}, of the initial and final states are calculated using the same set of solvent permanent charges; those equilibrated with the initial state. In adiabatic transitions the solvent structure changes during the transition and ΔG_{sol} takes a finite value. In this case the E_{int}^{pol} terms are calculated using two different set of solvent permanent charges.

The final scheme proposed for the determination of the transition energies and solvent shift with polarizable solvent is the following:

(1) The geometries and wave functions of the in solution initial and final states of the solute are calculated using a nonpolarizable solvent.

(2) Using the solvent configurations obtained in step 1 for the ground and excited states, the solute charge distribution and the induced solvent dipoles are equilibrated for each state separately. The ΔE_{solute} term is calculated with eq 4.

(3) The solute−solvent interaction energy with polarizable solvent, E_{int}^{pol}, for the ground and excited states are calculated with the aid of the eq 8. Next, ΔE_{int}^{pol} is calculated.

(4) For an adiabatic transition, the ΔG_{int} term is calculated using the FEP method. By difference with ΔE_{int}^{pol}, one obtains ΔG_{sol}. For vertical transitions, $\Delta G_{sol} = 0$ and $\Delta G_{int} = \Delta E_{int}^{pol}$.

(5) The transition energies and solvent shift are calculated using eqs 9 and 10, respectively.

Indirect Calculation of the Free Energy during the Adiabatic Transitions. In the case of adiabatic transitions, the ΔG_{sol} term must be calculated using FEP or thermodynamic integration (TI), with the problems and computational cost associated to the determination of free-energy differences. In this section we propose an alternative way to calculate adiabatic transition energies which avoids the calculation of ΔG_{sol}. The adiabatic transition value is calculated from the values of the absorption and emission vertical energies, assuming a linear response regime for the solvent.

In what follows and for the sake of clarity, we name the different states involved (see Figure 1). Structure 1 is the minimum of the ground state, structure 2 is the Franck−Condon point on the excited state, structure 3 is the minimum of the excited state, and structure 4 is the Franck−Condon point on the ground state.

In structures 1 and 3, we suppose that the solute and the solvent are completely relaxed, that is, the solvent is in equilibrium with the charge distribution of the solute molecule when this has reached its minimum, whereas structures 2 and 4 are characterized by nonequilibrium solvation, i.e., in these points the solvent is in equilibrium with the solute charge distribution of the structures 1 and 3, respectively.

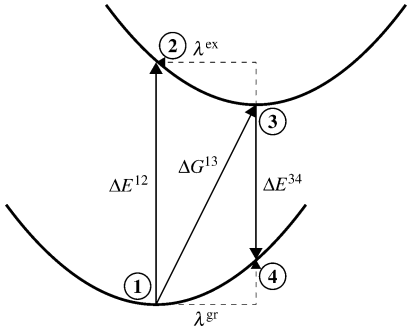

Figure 1. Electron transitions scheme.

The energy difference between structures 2 and 3 or between structures 4 and 1 is termed the reorganization energy. This energy is the sum of two contributions: one due to the reorganization of the solute geometry, λ_i, and other to the reorganization of the solvent structure around the solute, λ_s. In general, it is supposed—linear solvent response regime—that λ_s takes the same value in the ground and in the excited state (see, for instance, Bader and Berne[17] and references therein); however, the solute contribution, λ_i, is different in the ground and excited states because it depends on the characteristics of each potential energy surface.

From Figure 1, it is easy to see that the following relations are fulfilled:

$$\Delta G^{13} = \Delta E^{12} - \lambda^{ex} = \Delta E^{12} - \lambda_i^{ex} - \lambda_s \quad (11)$$

$$\Delta G^{13} = \Delta E^{43} + \lambda^{gr} = \Delta E^{43} + \lambda_i^{gr} + \lambda_s \quad (12)$$

By combining these two equations we get the following relations:

$$\lambda_s = \frac{1}{2}(\Delta E^{12} - \Delta E^{43}) - \frac{1}{2}(\lambda_i^{ex} + \lambda_i^{gr}) \quad (13)$$

and

$$\Delta G^{13} = \frac{1}{2}(\Delta E^{12} + \Delta E^{43}) + \frac{1}{2}(\lambda_i^{gr} - \lambda_i^{ex}) \quad (14)$$

The last term of eq 14, the difference between the solute relaxation in the ground and excited state, does not appear in most of the expressions proposed in the literature.[19] It is often supposed that the solute relaxation is the same in the ground and the excited states; however, as it is shown below, this assumption is not, in general, fulfilled, and this term can contribute significantly to the final energy. The solute relaxation energy can be easily calculated as the difference between them:

$$\lambda_i^{ex} = \langle \Psi^{(2)} | \hat{H}_{QM} | \Psi^{(2)} \rangle - \langle \Psi^{(3)} | \hat{H}_{QM} | \Psi^{(3)} \rangle \quad (15)$$

With an equivalent expression for the ground state changing the states 2 and 3 by 4 and 1, respectively. Sometimes, it is convenient to split λ_s into two terms, $\lambda_s = \Delta E_{int} + \Delta G_{sol}$, with similar meanings to those indicated in the previous section but where now the initial and final states are defined on the same free energy surface.

Computational Details. We applied the ASEP/MD methodology to study the $^1(n \rightarrow \pi^*)$ transition in the s-*trans*-acrolein

molecule. Ground and excited states were described using the CASSCF level of theory with dynamic correlation energy calculated with second-order perturbation theory (CASPT2). The complete active space is spanned by all the configurations arising from six valence electrons in five orbitals (6e/5o). Contracted basis functions based on atomic natural orbitals[20] (ANO) were used in the calculations. The contraction scheme used was C,O [4s3p1d]/H [2s1p]. The initial geometry for acrolein was obtained by CASSCF optimization, in vacuo, with the aforementioned basis set.

The MD simulations were performed using MOLDY.[21] The solvent was represented by 214 TIP3P[22] water molecules at fixed intramolecular geometry in a cubic box. The volume of the box was determined by the experimental density of water at 298 K (18.7 Å). These conditions have been proved to guarantee the correct description of the short range interaction. No significant changes where found when a larger number of solvent molecules were included in the MD simulation. In addition, periodic boundary conditions were applied and spherical cutoffs were used to truncate the intermolecular interactions at 9 Å. The long-range electrostatic interaction was calculated using the Ewald sum technique. The solute parameters were obtained by combining Lennard-Jones interatomic interactions[23] with electrostatic interactions. The temperature was fixed at 298 K by using the Nosé−Hoover[24] thermostat. Each simulation was run for 150 000 time steps where 50 000 were employed for equilibration and the 100 000 for production. A time step of 0.5 fs was used.

The free-energy perturbation method[17] was used to determine the ΔG_{int} energy. The solute geometry was assumed to be rigid and a function of the perturbation parameter (γ) and the solvent intramolecular geometry was considered always fixed. When $\gamma = 0$, the solute geometry and charges correspond to the initial state. When $\gamma = 1$, the charges and geometry are those of the final state. A linear interpolation is applied for intermediate values. A value of $\Delta\gamma = 0.05$ was used. That means that a total of 21 separate molecular dynamics simulations were carried out to determine the free-energy difference. To test the convergence of the calculation, the difference in interaction free energies calculated forward and backward was compared. For all the results reported below, the backward and forward free energies agree to within less than 5%.

During the ASEP/MD self-consistent process, the quantum calculations were performed at the CASSCF level of theory using the GAUSSIAN98 package[25] of programs. However, it is known[26] that to correctly describe electron transitions in conjugated molecules one must include the dynamic correlation contribution. Hence, once the solvent structure around the solute was obtained, we used the CASPT2 method included in MOLCAS-5[27] to recalculate the transition energies and solvent shift values.

The ASEP/MD self-consistent process was run over 10 quantum-calculation−molecular-dynamics simulation cycles. Even though only four or five cycles were needed to achieve the convergence in solute charges, the procedure was continued during 10 cycles. In this way, the final results with their statistical errors can be obtained as average of the last five cycles.

Results

To facilitate the discussion of the results, we have divided this section in two parts. The first one is dedicated to the description of the solvent effects on the geometry of the $^1(n \rightarrow \pi^*)$ excited stated of acrolein and on the solvent structure around it. The second one describes the energetic relations between the different points of the ground and excited free energy surface. All data refers to the s-*trans*-conformer.

TABLE 1: Some Bond Distances (in Å) of Acrolein in Vacuo and in Solution for the Ground and Excited States

	C=C	C−C	C=O
S_0 vac	1.340	1.473	1.204
S_0 sol	1.339	1.464	1.210
S_1 vac	1.398	1.371	1.354
S_1 sol	1.399	1.370	1.357

TABLE 2: Dipole Moments (in D) In Vacuo and in Solution Calculated at Different Points of the Free-Energy Surfaces (see Figure 1)

	1	2	3	4
μ^0	3.03	0.91	1.45	3.53
μ	3.98 ± 0.05	1.79 ± 0.09	1.72 ± 0.07	4.10 ± 0.09

Solute and Solvent Structure. Table 1 displays the geometry of the $^1(n \rightarrow \pi^*)$ excited state, structure (3), of the acrolein molecule in vacuo and in solution. In both cases, the two structures were characterized as real minima through the study of the Hessian matrix. The solvent effect on the geometry is very small; it produces a slight shortening of the two C−C distances while the C−O distance increases. This behavior is compatible with the formation of a hydrogen bond between the carbonyl oxygen of acrolein and the hydrogen of the water molecules. This trend agrees satisfactorily with the results found when continuum solvation models are employed.[10b] The small effect of the solvent on the excited-state contrasts with that found in the ground state, structure 1, where the solvent had a stronger influence on the geometry (the trends are the same but the magnitude of the changes are larger). This weaker influence of the solvent on the excited-state geometry is due to the lower solute−solvent interaction energy in the excited-state with respect to the ground state, which will be discussed below.

Table 2 displays the dipole moment values for the four structures considered. The $^1(n \rightarrow \pi^*)$ excitation is accompanied by a charge flux from the carbonyl bond to the carbon skeleton, this flux decreases the dipole moment of the excited-state with respect to the ground state value, and originates the lowering of the solute−solvent interaction energy. As expected, the solvent favors the charge separation in the solute molecule increasing the dipole moment value, however, the charge flux during the excitation is almost the same in gas phase and in solution, as evidenced when one compares the difference in the dipole moment of ground and excited states in the two phases. It is striking that, in vacuo, structure 2 has a lower dipole moment than structure 3; however, the contrary is found in solution. The explanation to this fact is that in solution the dipole moment of structure 2 is calculated in the presence of the reaction potential in equilibrium with the ground state. This reaction potential is larger than the one used in the calculation of structure 3 where the solvent is in equilibrium with the charge distribution of the excited state. As a consequence, the solvent polarizes more structure 2 and yields a larger value of the induced dipole moment.

The charge flux that accompanies the electron transition has also an influence on the solvent structure around the excited-state of the acrolein molecule, structure 3. Figures 2 and 3 display the O(acrolein)−O(water) and O(acrolein)−H(water) radial pair distribution function (rdf) in the ground and excited states (1 and 3). In the O−O rdf, the height of the first peak decreases with the excitation and its position is shifted to longer distances, the same is valid for the rest of the peaks, the solvent

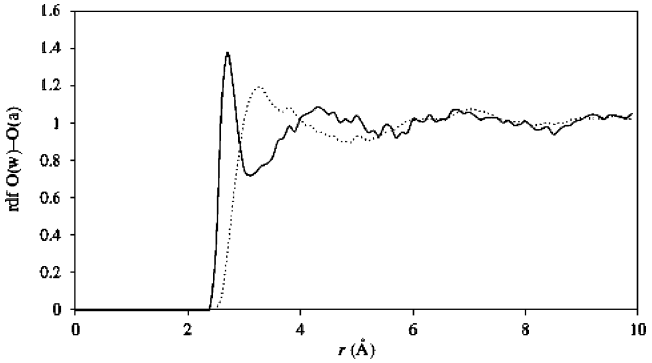

Figure 2. O(acrolein)−O(water) rdf for the ground (full line) and excited states (dotted line).

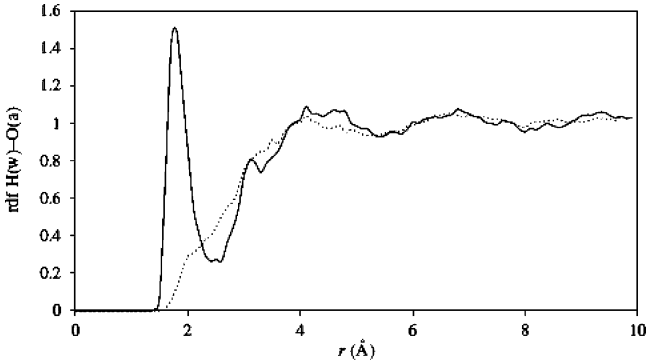

Figure 3. O(acrolein)−H(water) rdf for the ground (full line) and excited states (dotted line).

TABLE 3: Absorption, Emission, and Adiabatic Transition Energies, in eV

	ΔE_{12}	ΔE_{34}	ΔG_{13}
vacuum (CASSCF)	3.97	2.26	3.16
vacuum (CASPT2)	3.77	2.47	3.10
solution non pol. (CASSCF)	4.17	2.28	3.26
solution pol. (CASSCF)	4.16	2.32	3.30
solution pol. (CASPT2)	3.96	2.54	3.28

is less structured around the excited-state than around the ground state. The number of solvent molecules included in the first solvation shell (calculated by integration until the first minimum of the ground state rdf) are 1.96 and 1.16 for the ground and excited state, respectively. The behavior of the O−H rdf is even more striking, the solvent structure found around the solute ground state is completely lost in the solute excited state. One can conclude that the $^1(n \rightarrow \pi^*)$ excitation produces the partial desolvation of acrolein. This desolvation determines the energetic features of the emission process in solution.

Energies. Table 3 shows the absorption and emission transition energies between the four structures considered in vacuum and in water solution, in this last case considering both polarizable and nonpolarizable solvent.

Regarding the in vacuo transitions, the CASPT2//CASSCF vertical absorption is found at 3.77 eV that compares very well with other theoretical results[10] and with the experimental values: 3.71 eV in vacuo[6a] and 3.75 in 2-methyltetrahydrofuran.[6c] The electronic band origin, calculated as the energy difference between the excited and the ground state at their respective optimized equilibrium geometries, is also well reproduced 3.10 eV obtained theoretically versus 3.21[6b]−3.31[6c] eV from the experiment. This value has been estimated in 3.12 eV by Aquilante et al. [10a] using a similar level of calculation. The good agreement between the calculated electronic band origin and the experimental data, permits us to conclude that the provided geometry of the relaxed excited-state in vacuo is essentially correct. The vertical emission transition predicted at CASPT2//CASSCF is 2.47 eV. There is no experimental data for the emission spectrum in vacuo. The fluorescence spectrum registered in 2-methyltetrahydrofuran solution[6c] shows a broad band at 3.00 eV. However, given the nonpolar nature of this solvent and the good agreement found between the absorption spectra in vacuo and in 2-methyltetrahydrofuran, we can consider that the maximum for the emission in such as solvent would not differ too much from the in vacuo value. Trying to check the quality of our calculation, CASPT2 geometry optimizations were performed for the excited-state using both (6e,5o) and (12e,11o) active spaces. CASPT2//CASPT2 vertical emission transitions where evaluated at these geometries but no relevant differences where found respect to the (6e,5o) CASPT2//CASSCF calculation. It is known that, in fluorescence spectra, the vertical transition does not necessarily coincide with the maximum of the band. A detailed analysis of the discrepancy found between the experimental emission maximum and the computed vertical transition implies the calculation of the Franck−Condon factors, something that is beyond of the scope of this paper.

Next, we pass to discuss the results in solution. We begin by analyzing the CASSCF//CASSCF results obtained with the nonpolarizable solvent model. Compared with the corresponding in vacuo transitions the solvent originates a shift of 4.6 kcal/mol in the absorption band and of 0.4 kcal/mol in the emission band of acrolein. The experimental solvent shift of the absorption band is 4.5 kcal/mol. Positive values indicate a blue shift. The different solvent shift value found between the absorption and emission process is related to the different strength of the solute-solvent interaction in the ground and excited states. As indicated above, the charge flux that accompanies the excitation yields a lower dipole moment, weaker solvent structure around the solute, and as a consequence, lower solute−solvent interaction energy (and energy differences) when the solvent is in equilibrium with the excited state. The band origin, $1 \rightarrow 3$ adiabatic transition, appears at 3.16 eV in vacuo and 3.26 eV in solution. This last result has been obtained using eq 14. The solvent blue shift is 2.3 kcal/mol, halfway between the magnitude of the solvent shift in the absorption and emission vertical transitions. The adiabatic transition can also be calculated using the FEP method. In this case, one obtains 3.32 eV, the slight discrepancy between the two methods is probably due, in part, to the approximations introduced in the calculation of the free energy with the FEP method, where the solute was classically represented and not quantum mechanically as it is done in eq 14 and, in part, to the breakdown of the linear solvent response regime approximation.

Now, we analyze the reorganization energies in the ground and excited states, that is, the energy difference between structures 4 and 1 and 2 and 3, respectively. In the excited-state the total reorganization energy is 20.9 kcal/mol, from this quantity 17.7 kcal/mol correspond to the relaxation in the solute geometry and 3.2 kcal/mol to the solvent reorganization. In the ground state, the reorganization energy is 22.6 kcal/mol that splits in 19.4 kcal/mol and 3.2 kcal/mol, respectively. In both the ground and excited-state the reorganization energy is dominated by the solute geometry relaxation contribution. As indicated above, the solvent reorganization energy can, in turn, be split into two terms, one associated to the difference in the solute−solvent interaction energies, and the other to the difference in the solvent distortion energy. In the excited state, these terms take the values −2.4 kcal/mol and 5.6 kcal/mol,

TABLE 4: Total Solvent Shift, δ, and Its Components (in kcal/mol) for the Absorption and Emission Processes (Polarizable Solvent)[a]

	$1/2\ \Delta U_{\mu q}$	$\Delta U_{\rho q}$	$1/2\ \Delta U_{\rho\mu}$	ΔE_{solute}	δ
absorption	0.04 ± 0.02	5.9 ± 0.4	1.1 ± 0.1	-2.7 ± 0.4	4.3 ± 0.2 (4.5 ± 0.2)
emission	0.01 ± 0.01	1.2 ± 0.3	0.7 ± 0.1	-0.7 ± 0.2	1.2 ± 0.3 (1.8 ± 0.3)

[a] Values in parentheses calculated at the CASPT2//CASSCF level.

respectively. Due to the larger value of the dipole moment, the solute−solvent interaction energy is larger in 2 than in 3. In the ground state, the solute−solvent interaction energy is larger in 1 than in 4 by 8.8 kcal/mol. The solvent distortion energy is −5.6 kcal/mol (the same, in absolute value, as in the excited state, since it depends only on the solvent coordinates). Finally, we note that the magnitude of the solute reorganization is slightly different in the ground and excited state, the difference between the two values is about 1.7 kcal/mol, its effect is to increase the adiabatic transition energy in about 0.8 kcal/mol, see eq 14.

When the solvent is considered polarizable, the CASPT2 solvent blue shifts are 4.5, 1.8, and 4.1 kcal/mol for the absorption, emission and adiabatic transition, respectively. Again, the adiabatic value was obtained by using eq 14. Continuum methods have also been employed in the calculation of the absorption solvent shift. In this way Andrade do Monte et al. [10b] obtained a value of 3.7 kcal/mol using the COSMO method and MR-CISD in solution optimized geometry. Using the PCM method and CASPT2 in vacuo optimized geometries Aquilante el al.[10a] obtained a solvent shift of 7.6 kcal/mol. The overestimate of the solvent shift calculated by those authors may in part be due to the use of geometries optimized in vacuo for the computation in solution, as we argued in previous studies.[12] The largest contribution to the solvent shift (Table 4) comes from the interaction between the solute charge distribution and the permanent charges of the solvent, $\Delta U_{\rho q}$. However, the contribution of the solvent polarization (induced dipoles) is also important, representing about 18% of the contribution of the permanent charges in the absorption process and 55% in the emission process. In the emission process, the value of this component compensates the energy spent in polarizing the solute charge distribution. The results obtained with polarizable solvent are similar to those obtained with an effective charges model, being the computational cost notably lower in the last case.

Finally, we shall make a few comments about the effect of the inclusion of the electron correlation calculated at CASPT2 level. The inclusion of the dynamic electron correlation increases the solvent shift in 0.2 kcal/mol in the absorption process and in 0.6 kcal/mol in the emission process. On a percentage basis, the contribution of the dynamic electron correlation to the solvent shift represents 33% of the total solvent shift in the emission process but less than 5% of the total solvent shift in the absorption process.

Conclusions

Solvation produces a blue shift on the $^1(n \rightarrow \pi^*)$ electron transition of acrolein in water, both in the absorption and emission spectra. The $^1(n \rightarrow \pi^*)$ excitation is accompanied by a charge flux from the oxygen to the carbon skeleton, this flux decreases the dipole moment of the excited-state with respect to the ground state value. At the same time it produces the partial desolvation of the excited state. These two effects destabilize the excited-state with respect to the ground state and explain the experimentally found blue shift.

Solvation also produces a shortening of the two C−C distances and an increase of the C−O distance. As a consequence of its larger solute−solvent interaction energies, these effects are larger in the ground state than in the excited state. We demonstrated that although the solvent polarization plays an important role in the description of the electron transition, especially in the case of the emission process, an effective charge representation of the solvent as given by TIP3P, for instance, yields similar results and is more economical from a computational point of view. The inclusion of the electron correlation calculated at CASPT2 level has only a small effect on the solvent shift in the absorption process but it makes a very important contribution to the solvent shift in the emission process.

Finally, we proposed a new method for calculating the transition free energy in adiabatic transitions once the values of the vertical absorption and emission electron transition energies are known. The method avoids the classical calculation of the free-energy difference between the ground and excited-state and permits to determine easily the position of the electronic band origin.

Acknowledgment. This research was sponsored by the Consejería de Educación, Ciencia y Tecnología (3PR05A105) and the Dirección General de Investigación Científica y Técnica (CTQ2004-05680)

References and Notes

(1) Reichardt, C. *Solvents and Solvent Effects in Organic Chemistry*, 2nd ed.; VCH: Weinheim, 1990.

(2) (a) Cembran, A.; González-Luque, R.; Altoè, P.; Merchán, M.; Bernardi, F.; Olivucci, M.; Garavelli, M. *J. Phys. Chem. A* **2005**, *109*, 6597 (b) Hufen, J.; Sugihara, M.; Buss, V. *J. Chem. Phys. B* **2004**, *108*, 20419. (c) Wanko, M.; Hoffman, M.; Strodel, P.; Koslowski, A.; Thiel, W.; Neese, F.; Frauenheim, T., Elstner M. *J. Phys. Chem. B* **2005**, *109*, 3606.

(3) (a) Tomasi, J.; Bonaccorsi, R.; Cammi, R.; Olivares del Valle, F. J. *J. Mol. Struct.* (*Theochem)* **1991**, *234*, 401. (b) Tomasi, J.; Persico, M. *Chem. Rev.* **1994**, *94*, 2027. (c) Rivail, J.-L.; Rinaldi, D. in *Computational Chemistry: Review of Current Trends*; Leszczynski, J., Ed.; World Scientific Publishing: Singapore, 1995. (d) Cramer, C. J.; Truhlar, D. G. in *Reviews in Computational Chemistry*; Lipkowitz, K. B.; Boyd, D. B., Eds.; VCH Publishers: New York, 1995; Vol. VI, p 1. (e) Klamt, A; Schüürmann, G. *J. Chem. Soc. Perkin Trans. II* **1993**, 799. (f) Truong, T. N.; Stefanovich, E. V. *Chem. Phys. Lett.* **1995**, *240*, 253.

(4) (a) Sánchez, M. L.; Martín, M. E.; Aguilar, M. A.; Olivares del Valle, F. J. *Chem. Phys. Lett.* **1999**, *310*, 195. (b) Martín, M. E.; Sánchez, M. L.; Olivares del Valle, F. J.; Aguilar, M. A. *J. Chem. Phys.* **2000**, *113*, 6308. (c) Martín, M. E.; Sánchez, M. L.; Aguilar, M. A.; Olivares del Valle, F. J. *J. Mol. Struct.: THEOCHEM*, **2001**, *537*, 231. (d) Muñoz Losa, A.; Fdez. Galván, I.; Martín, M. E.; Aguilar, M. A. *J. Phys. Chem. B* **2006**, *110*, 18064.

(5) (a) Sánchez, M. L.; Aguilar, M. A.; Olivares del Valle, F. J. *J. Comput. Chem*., **1997**, *18*, 313. (b) Sánchez, M. L.; Martín, M. E.; Aguilar, M. A.; Olivares del Valle, F. J. *J. Comput. Chem*. **2000**, *21*, 705. (c) Muñoz Losa, A; Fdez. Galván, I.; Martín, M. E.; Aguilar, M. A. *J. Phys. Chem. B* **2003**, *107*, 5043. (d) Sánchez, M. L.; Martín, M. E.; Fdez. Galván, I.; Olivares del Valle, F. J.; Aguilar, M. A. *J. Phys. Chem. B* **2002**, *106*, 4813. (e) Fdez. Galván, I; Sánchez, M. L.; Martín, M. E.; Olivares del Valle, F. J.; Aguilar, M. A. *Comput. Phys. Commun.* **2003**, *155*, 244.

(6) (a) Brand, J. C. D.; Williamson, D. G. *Discuss. Faraday Soc.* **1963**, *35*, 184. (b) Hollas, J. M. *Spectrochim. Acta* **1963**, *19*, 1425. (c) Becker, R. S.; Inuzuka, K.; King, J. *J. Chem. Phys.* **1970**, *52*, 5164. (d) Osborne, G. A.; Ramsay, D. A. *Can. J. Phys.* **1973**, *51*, 469. (e) Moskvin, A. E. *Theor. Exp. Chem.* **1966**, *2*, 175. e) Walsh, A. D. *Trans. Faraday Soc.* **1945**, *41*, 498.

(7) (a) Davidson, E. R.; Nitzsche, L. E. *J. Am. Chem. Soc.* **1979**, *101*, 6524. (b) Valenta, K.; Grein, F. *Can. J. Chem.* **1982**, *60*, 601. (c) Dykstra, C. E. *J. Am. Chem. Soc.* **1976**, *98*, 7182. (d) Devaquet, A. *J. Am. Chem. Soc.* **1972**, *94*, 5160. (e) Reguero, M.; Olivucci, M.; Bernardi, F.; Robb, M. A. *J. Am. Chem. Soc.* **1993**, *115*, 3710. (f) Saha, B.; Ehara, M., Nakatsuji, H. *J. Chem. Phys.* **2006**, *125*, 014316.

(8) (a) Fridh, C.; Åsbrink, L.; Lindholm, E. *Phys. Scr.* **1979**, *20*, 603. (b) Haque, W. *J. Chem. Phys.* **1977**, *67*, 3629. (c) Thakur, S.; Gupta, V. P.; Ram, B. *Spectrochim. Acta A* **1997**, *53*, 749.

(9) Ten-no, S.; Hirata, F.; Kato, S. *J. Chem. Phys*. **1994**, *100*, 7443.

(10) (a) Aquilante, F.; Barone, V.; Roos, B. O. *J. Chem. Phys.* **2003**, *119*, 12323. (b) Andrade do Monte, S.; Müller, T.; Dallos, M.; Lischka, H.; Diedenhofen, M.; Klamt, A. *Theor. Chem. Acc*. **2004**, *111*, 78.

(11) (a) Brancato, G.; Rega, N.; Barone, V. *J. Chem. Phys*. **2006**, *125*, 164515. (b) Georg, H. C.; Coutinho, K.; Canuto, S. *J. Chem. Phys*. **2005**, *123*, 124307.

(12) Martín, M. E.; Muñoz Losa, A.; Fdez. Galván, I.; Aguilar, M. A. *J. Chem. Phys.* **2004**, *121*, 3710.

(13) Caricato, M.; Mennucci, B.; Tomasi, J.; Ingrosso, F.; Cammi, R.; Corni, S.; Scalmani, G. *J. Chem. Phys.* **2006**, *124*, 124520.

(14) Fdez. Galván, I.; Sánchez, M. L.; Martín, M. E.; Olivares del Valle, F. J.; Aguilar, M. A. *J. Chem. Phys.* **2003**, *118*, 255.

(15) (a) Okuyama-Yoshida, N.; Nagaoka, M.; Yamabe, T. *Int. J. Quantum Chem.* **1998**, *70*, 95. (b) Okuyama-Yoshida, N.; Kataoka, K.; Nagaoka, M.; Yamabe, T. *J. Chem. Phys*. **2000**, *113*, 3519. (c) Hirao, H.; Nagae, Y., Nagaoka, M. *Chem. Phys. Lett*. **2001**, *348*, 350.

(16) (a) Chandrasekhar, J.; Smith, S. F.; Jorgensen, W. L. *J. Am. Chem. Soc*. **1985**, *107*, 154. (b) Chandrasekhar, J.; Jorgensen, W. L. *J. Am. Chem. Soc*. **1985**, *107*, 2974. (c) Jorgensen, W. L. *Acc. Chem. Res*. **1989**, *22*, 184.

(17) (a) Debolt, S. E.; Kollman, P. A. *J. Am. Chem. Soc*. **1990**, *112*, 7515. (b) Kollman, P. A. *Chem. Rev*. **1993**, *93*, 2395. (c) Mark, A. E. in *Encyclopedia of Computational Chemistry*; Schleyer, P. V. R., Allinger, N. L., Clark, T., Gasteiger, J., Kollman, P. A., Schaefer, H. F., III, Schreiner, P. R., Eds.; Wiley and Sons: Chichester, 1998; Vol. 2., p 1070.

(18) (a) Aguilar, M. A.; Olivares del Valle, F. J.; Tomasi, J. *J. Chem. Phys.* **1993**, *98*, 7375. (b) Aguilar, M. A. *J. Phys. Chem. A* 105, **2001**, 10393. (c) Menucci, B.; Cammi, R.; Tomasi, J. *J. Chem. Phys.* **1998**, *109*, 2798. (e) Cammi, R.; Menucci, B. *J. Chem. Phys.* **1999**, *110*, 9877. (f) Cammi, R.; Menucci, B.; Tomasi, J. *J. Phys Chem.* A **2000**, *104*, 5631. (g) Cossi, M.; Barone, V., *J. Chem. Phys.* **2001**, *115*, 4708.

(19) Bader, J. S.; Berne, B. J. *J. Chem. Phys*. **1996**, *104*, 1293.

(20) Widmark, P.-O.; Malmqvist, P.-Å.; Roos, B. O. *Theor. Chim. Acta* **1990**, *77*, 291.

(21) Refson, K. *Comput. Phys. Commun.* **2000**, *126*, 310.

(22) Jorgensen, W. L.; Chandrasekhar, J.; Madura, J. D.; Impey, R. W.; Klein, M. L. *J. Chem. Phys.* **1983**, *79*, 926.

(23) Jorgensen, W. L.; Maxwell, D. S.; Tirado-Rives, J. *J. Am. Chem. Soc*. **1996**, *117*, 11225.

(24) Hoover, W. G. *Phys. Rev. A* **1985**, *31*, 1.

(25) Frisch, M. J.; Trucks, G. W.; Schlegel, H. B.; Scuseria, G. E.; Robb, M. A.; Cheeseman, J. R.; Zakrzewski, V. G.; Montgomery, J. A., Jr.; Stratmann, R. E.; Burant, J. C.; Dapprich, S.; Millam, J. M.; Daniels, A. D.; Kudin, K. N.; Strain, M. C.; Farkas, O.; Tomasi, J.; Barone, V.; Cossi, M.; Cammi, R.; Mennucci, B.; Pomelli, C.; Adamo, C.; Clifford, S.; Ochterski, J.; Petersson, G. A.; Ayala, P. Y.; Cui, Q.; Morokuma, K.; Malick, D. K.; Rabuck, A. D.; Raghavachari, K.; Foresman, J. B.; Cioslowski, J.; Ortiz, J. V.; Stefanov, B. B.; Liu, G.; Liashenko, A.; Piskorz, P.; Komaromi, I.; Gomperts, R.; Martin, R. L.; Fox, D. J.; Keith, T.; Al-Laham, M. A.; Peng, C. Y.; Nanayakkara, A.; Gonzalez, C.; Challacombe, M.; Gill, P. M. W.; Johnson, B. G.; Chen, W.; Wong, M. W.; Andres, J. L.; Head-Gordon, M.; Replogle, E. S.; Pople, J. A. *Gaussian 98*, revision A11.3; Gaussian, Inc.: Pittsburgh, PA, 1998.

(26) Molina, V.; Merchán, M. *J. Phys. Chem*. **2001**, *105*, 3745.

(27) Andersson, K.; Barysz, M.; Bernhardsson, A.; Blomberg, M. R. A.; Carissan, Y.; Cooper, D. L.; Cossi, M.; Fleig, T.; Fülscher, M. P.; Gagliardi, L.; de Graaf, C.; Hess, B. A.; Karlström, G.; Lindh, R.; Malmqvist, P.-Å.; Neogrády, P.; Olsen, J.; Roos, B. O.; Schimmelpfennig, B.; Schütz, M.; Seijo, L.; Serrano-Andrés, L.; Siegbahn, P. E. M.; Stalring, J.; Thorsteinsson, T.; Veryazov, V.; Wierzbowska, M.; Widmark, P.-O., MOLCAS Version 5.2, University of Lund, Lund, Sweden, 2003.